

Thermo-Economic Assessment and Optimization of Actual Heat Engine Performance by Implementation of NSGA II

M. Ghazvini^{1*}, S.M. Pourkiaei² and F. Pourfayaz²

1. Department of Ocean and Mechanical Engineering, Florida Atlantic University, 777 Glades Road Boca Raton, FL 33431, USA.
2. Department of Renewable Energies, Faculty of New Sciences and Technologies, University of Tehran, Tehran, Iran.

Receive Date 11 May 2020; Revised 15 May 2020; Accepted Date 26 May 2020
*Corresponding author: mghazvini2020@fau.edu (M. Ghazvini)

Abstract

Finding a superior evaluation of an irreversible actual heat engine (irreversible Carnot heat engine) can be mentioned as the substantial purpose of this work. The considered criteria are Ecological Coefficient of Performance (ECOP), exergetic performance coefficient thermo-economic, ecological-based thermo-economic, and ecologico-economical functions. These criteria are optimized by implementing NSGA II and thermodynamic analysis. The irreversibility of the system is considered for the work assessment, and consequently, two states are specified in the optimization procedure. The findings associated with every scheme are assessed independently. In the first scenario, maximizing the power output, the first law efficiency of the system, and the dimensionless ecological-based thermo-economic function (f_E) are set as the target. In the second scenario, the three objective functions power output (\dot{W}), efficiency (η), and dimensionless ecologico-economical (f_{EC}) are simultaneously maximized. To be clear, the coupled multi-objective evolutionary approaches (MOEAs) and non-dominated sorting genetic algorithm (NSGA-II) approach are presented. Comparison of the three prominent approaches LINAMP, TOPSIS, and FUZZY is performed in decision-making. Ultimately, error analysis of the results based on the maximum absolute percentage error is carried out. According to the results obtained, in the first scenario, the appropriate results are the result of the decisions made by TOPSIS and LINAMP with a deviation index equal to 0.322 from the ideal ratio of this scenario. In the second scenario, the best decision-making results are achieved by the TOPSIS method with a deviation index equal to 0.104 from the ideal state for this scenario.

Keywords: Ecological coefficient of performance; Ecological-based thermo-economic function; Exergetic performance coefficient thermo-economic; Optimization; Decision-making.

1. Introduction

Optimization of thermal systems is now one of the main characters of energy management [1–8] due to the non-renewable energy resource, environmental pollution, and costs. As the Carnot cycle is an ideal reversible system, it provides the highest amount of efficiency and work output. This ideal model provides an investigation of the actual system performance under the effect of irreversibilities [9]. Novikov [10] and Curzon and Ahlborn [11] have presented a novel cycle considering external irreversibilities. They presented the first endo-reversible heat engine. The irreversibilities of this kind of engines are caused by heat transfer. Many optimizations have been done for various thermodynamic cycles using the finite time thermodynamic (FTT) method; the references [12–18] present a number of them. One

of the common methods named ecological function was firstly presented by Angulo Brown [19]. This function describes $E = \dot{W} - T_L \dot{S}_{gen}$; E alleviates the entropy generation and modifies the power output up to 10% in comparison with the Curzon–Ahlborn engine [19]. Yan has remodeled this presentation as $E = \dot{W} - T_0 \dot{S}_{gen}$ [20]. Emin Açıkkalp [21] has investigated the thermodynamic optimization criteria for the actual power generating thermal cycles, reporting that the ecological function criterion is the most suitable optimization method among the other methods for an irreversible Carnot cycle. Açıkkalp has also evaluated the exergetic sustainability index for an irreversible Carnot refrigerator [22]. Gülcan Özel [23] has evaluated four different thermo-environmental criteria for an actual heat engine. He

has reported the ecologico-environmental method as the most convenient thermo-environmental method among the other methods. He has also reported the ecologico-economic criteria as the key thermo-economic ones for an irreversible Carnot heat engine [24]. Chen has selected power output along with efficiency as the objective functions, and has examined the heat engine's optimum performance [25]. Ozcaynak *et al.* have investigated an internal irreversible radiative heat engine by the FTT approach. They introduced the cycle-irreversibility parameter R as the key character of the radiative heat engine [26]. Cheng and Chen have employed ecological optimization considering the finite thermal capacitance rates [27]. Some more comprehensive works are Xia [28], Chen [29], and Zhu and colleagues. [30]. Ibrahim *et al.* have introduced the "coefficient of irreversibility" in order to consider the internal irreversibilities [31]. De Vos [32] has presented a mathematical thermo-economical design of an endo-reversible heat engine. Sahin and Kodal [33] have investigated an endo-reversible heat engine and a heat pump utilizing the refrigerator cooling and heat pump heating as the objective functions. The references [34–37] are some research works that have employed the thermo-economic and exergoeconomic approaches. The ecological-based thermo-economic function is a different thermo-economic standard represented by Barranco-Jimenez [38]. This function defines the heat engine thermo-economic performance of its highest ecological states. In the references [34–37], the economic criteria entitled ecologico-economical function are reviewed. Still, a comprehensive examination of the ecologico-economical function has not been performed yet.

A number of studies can be found in the literature on the subject of ecological optimization [39–41]. ECOP has been utilized for different systems [42–44]. In order to establish a correlation between exergy and exergy destruction in a system, a performance coefficient entitled Exergetic Performance Criteria (EPC) was presented [45, 46]. Several investigations of exergy by finite-time thermodynamics (FTT) could be found in the references [47, 48].

A multi-objective optimization is a reliable approach for thermodynamic studies [49–51]. In order to solve this kind of problem, the evolutionary algorithm (EA) has been presented since the 20th century [52]. In these types of problems, the intention is to obtain a collection of paths so that the objective functions are applied for each solution in an almost important procedure [52]. The outcome is a large collection of answers

called Pareto frontier, presenting the probable answers all through the function zone. This method has generally been utilized in many studies [37, 53–56].

In [53, 54], using the evolutionary algorithms, a creative approach is improved for the objective of determining the power of the solar Stirling heat engine. A thermo-economic optimization of the Stirling heat pump has been presented in [56], employing NSGA-II.

In the present research work, two optimization states are presented for the actual heat engine cycle. In the first scenario, maximizing the power output (\dot{W}), the first law efficiency of the system and the dimensionless ecological-based thermo-economic function (f_E) are set as the target. The three objective functions to be maximized in the next scenario are power output (\dot{W}), efficiency (η), and dimensionless ecologico-economical (f_{EC}). The uniqueness of this work is for presenting the coupled multi-objective evolutionary approaches (MOEAs) and non-dominated sorting genetic algorithm (NSGA-II) approach on a system.

2. Thermodynamic study

During this research work, an irreversible Carnot heat engine is studied. The studied model design is shown in figure 1. The heat sink and heat source are supposed to be infinite. TH, TL, TE, and TC are the heat source, heat sink, evaporator, and condenser temperature, respectively.

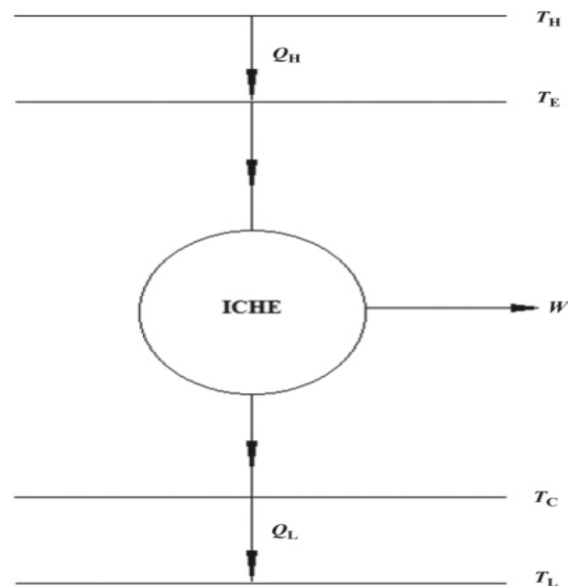


Figure 1. Diagram of irreversible Carnot heat engine (ICHE).

The heat input is as follows (kW):

$$Q_H = \alpha(T_H - T_E) \tag{1}$$

in which α expresses the heat conductance of the hot side (kW/K). The system heat rejection (kW) can be provided as follows:

$$\dot{Q}_L = \beta(T_C - T_L) \quad (2)$$

in which β indicates the heat conductance of the cold side (kW/K). According to the first law of thermodynamics, the power output of the system is as follows:

$$\dot{W} = \dot{Q}_H - \dot{Q}_L \quad (3)$$

Equation (4) represents the Clausius inequality derived by the second law of thermodynamics:

$$\frac{\dot{Q}_H}{T_E} - \frac{\dot{Q}_L}{T_C} \leq 0 \quad (4)$$

By applying the internal irreversibility parameter (I) that is dimensionless, inequality can be expressed as equality. The heat engine is endoreversible and internally irreversible when $I = 1$ and $I > 1$, respectively [31]:

$$I \frac{\dot{Q}_H}{T_E} = \frac{\dot{Q}_L}{T_C} \quad (5)$$

Irreversibilities of the system are measured by the exergy destruction rate, which can be calculated like:

$$Ex_D = T_0 \left(\frac{\dot{Q}_L}{T_L} - \frac{\dot{Q}_H}{T_H} \right) \quad (6)$$

The system first law efficiency can be calculated as follows:

$$\eta = \frac{\dot{W}}{\dot{Q}_H} = 1 - \frac{I}{x} \quad (7)$$

The ecological function (kW) can be determined by:

$$ECF = \dot{W} - Ex_D \quad (8)$$

The cost associated with the per-unit work output described as the thermo-economic function (kW/\$) is:

$$F = \frac{\dot{W}}{c_1 m + c_2 \dot{Q}_H + c_3 Ex_D + c_4 \dot{W}} \quad (9)$$

where m is the required total heat transfer area (m^2) of the system; and c_1 , c_2 , and c_3 are the capital, fuel, and environmental costs (\$/kW), respectively. c_4 (\$/kW) is also defined as:

$$c_4 = c_5 + c_6 \quad (10)$$

where c_5 expresses the capital recovery factor multiplied by the investment cost per unit power output (\$/kW) and c_6 is the maintenance as well as the operation cost (\$/kW). The ecological-based thermo-economic function (kW/\$) is determined as well [38]:

$$F_E = \frac{ECF}{c_1 m + c_2 \dot{Q}_H + c_3 Ex_D + c_4 \dot{W}} \quad (11)$$

In this method, the cost of the ecological function is taken into account, which makes it possible to

reach a minimum difference between the lost work costs and the power output. The ecologico-economical function is defined as:

$$F_{EC} = c_5 \dot{W} - c_3 Ex_D \quad (12)$$

Throughout the techniques in the references [34, 38], the thermodynamic examinations were performed (equations (13)–(17)):

$$x = \frac{T_E}{T_C} \quad (13)$$

$$y = \frac{\alpha}{\beta} \quad (14)$$

$$z = \alpha + \beta \quad (15)$$

$$T_E = \frac{(T_H I_y + x T_L)}{(1 + I_y)} \quad (16)$$

$$\dot{Q}_H = \frac{yz(T_H - x T_L)}{(1 + y)(1 + I_y)} \quad (17)$$

The dimensionless ecological-based thermo-economic and dimensionless ecologico-economical, respectively, can be presented as follow:

$$f_E = F_E c_4 \quad (18)$$

$$f_{EC} = \frac{F_{EC}}{W c_4} \quad (19)$$

3. Multi-objective optimization

As mentioned earlier, for the aim of optimizing the actual heat engine system, the multi-objective optimization was applied through EA in order to evaluate the preceding parameters of the cycle using the genetic algorithm (GA) tools. The following figure shows a schematic representation of GAs.

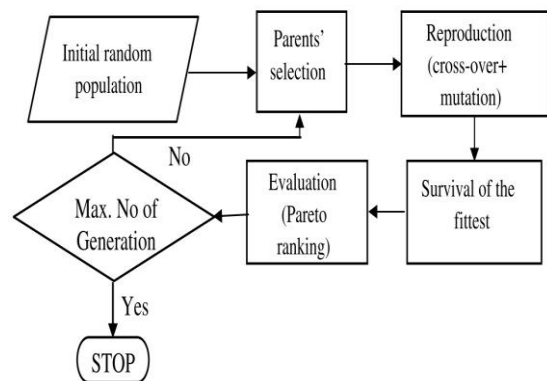


Figure 2. Multi-objective EA algorithm [57, 58].

3.1. Objective functions, decision variables, and constraints

The objective functions of the first state comprising power output, efficiency, and (f_E) are described by

equations (3, 7, and 18).

The objective functions of the next state comprising power output, efficiency, and (f_{EC}) are described by equations (3, 7, and 19).

The four chosen decision variables in our investigations are:

x : fluid temperature ratio ($x = \frac{T_E}{T_C}$),

y : parameter of the heat conductance rate ($y = \frac{\alpha}{\beta}$),

z : sum of heat conductance rate ($z = \alpha + \beta$),

τ : temperature ratio.

Each one of the decision parameters should be in a proper interval, even though they would be diverse in the optimization process. In order to achieve the objective functions, the following constraints are considered:

$$1 \leq y \leq 2 \tag{20}$$

$$1 \leq z \leq 20 \tag{21}$$

$$1 \leq x \leq 5 \tag{22}$$

$$3 \leq \tau \leq 6 \tag{23}$$

3.2. Multi-objective optimization decision-making

With the purpose of collecting the finest optimal path from the available paths within the multi-objective optimization methods, decision-making is essential. The decision-making approaches are implemented to select a superior optimal path from the Pareto frontier. Euclidean non-dimensionalization and fuzzy non-dimensionalization are two methods of non-dimensionalization.

3.2.1. Non-dimensionalization methods

3.2.1.1. Euclidean non-dimensionalization

F_{ij}^n is the objective matrix of different Pareto frontier solutions, which can be calculated as follows:

$$F_{ij}^n = \frac{F_{ij}}{\sqrt{\sum_{i=1}^m (F_{ij}^2)}} \tag{24}$$

3.2.1.2. Fuzzy non-dimensionalization

Throughout this approach, a non-dimensioned objective, F_{ij}^n , can be determined as below:

$$F_{ij}^n = \frac{F_{ij} - \min(F_{ij})}{\max(F_{ij}) - \min(F_{ij})} \text{ (maximization)} \tag{25a}$$

$$F_{ij}^n = \frac{\max(F_{ij}) - F_{ij}}{\max(F_{ij}) - \min(F_{ij})} \text{ (minimization)} \tag{25b}$$

The most renowned kind of decision-making approaches like LINMAP, TOPSIS, and fuzzy Bellman-Zadeh are applied for the aim of providing the optimal response during this assessment. To be clear, LINMAP and TOPSIS use

the Euclidean non-dimensionalization, whereas the latter approach uses fuzzy non-dimensionalization.

3.3. Decision-making approaches

3.3.1. Bellman-Zadeh approach

In the Bellman-Zadeh approach, defining the connection of all fuzzy norms and constrains is examined as the final decision. The details for the methods of ascertainment for the membership function are presented in [57, 58].

3.3.2. LINMAP approach

In the LINMAP decision-making approach, the “ideal point” can be considered as the point on the Pareto frontier where every objective is optimized regardless of taking the other objectives into account. The optimized amount of objectives could not be equivalent in any case. Therefore, the stated ideal data point is not positioned on the Pareto frontier. Lastly, the nearest route to an ideal data point in space is considered as a preceding optimum route. The references [57, 58] provide more details of the procedure.

3.3.3. TOPSIS approach

In accordance with the TOPSIS decision-making approach, a “non-ideal point” that is determined as the latitude all over the objective spatial is presented. The longest and shortest spacings by the non-ideal point are simultaneously chosen as the last path. The references [57, 58] provide more details for the procedure.

4. Results and discussion

In this part, the analyzed system’s results are presented. The examination characters of the study are listed in table 1.

As depicted in figure 3, increasing the ratio of fluid temperature (x) leads to an increase in the dimensionless ecologico-economical. It should be noticed that enhancing the temperature ratio (τ) leads to an increase in the exergy destruction and the work losses, and as a result, the dimensionless ecologico-economical decreases.

As presented in figure 4, the power output (W) enhances with the enhancement of the ratio of fluid temperature (x) till the power output (W) is obtained, and subsequently, reduces with the enhancement of the fluid temperature ratio (x). It should be noticed that the heat entering the system increases, and as a result, the power output increases as well by increasing the temperature ratio (τ).

Table 1. Parameters of the assessment.

Parameter	Unit	Value
T_L	K	300
T_0	K	298.15
I	-	1.05
c_1	\$/m ²	10
c_2	\$/kW	100
c_3	\$/kW	2
c_5	\$/kW	5
c_6	\$/kW	2
c_7	\$/kW	6
m	m ²	1000

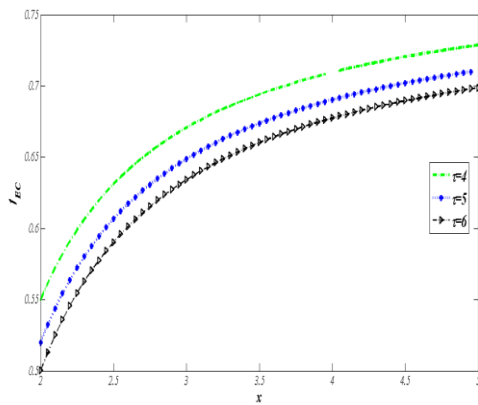


Figure 3. Fluid temperature ratio (x) at various values of the temperature ratio (τ) on the dimensionless ecological-economic in ($z=10, y=2$).

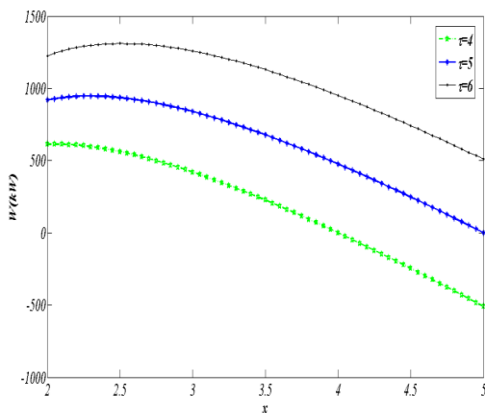


Figure 4. Effects of the ratio of fluid temperature (x) at various values of the temperature ratio (τ) on the power output in ($z=10, y=2$).

As shown in figure 5, f_{EC} enhances by enhancing the fluid temperature ratio. Conversely, as depicted

in Figure 5, decreasing and/or increasing the value of the sum of heat conductance rate (Z) is not effective on the amount of the ecological-economic (f_{EC}).

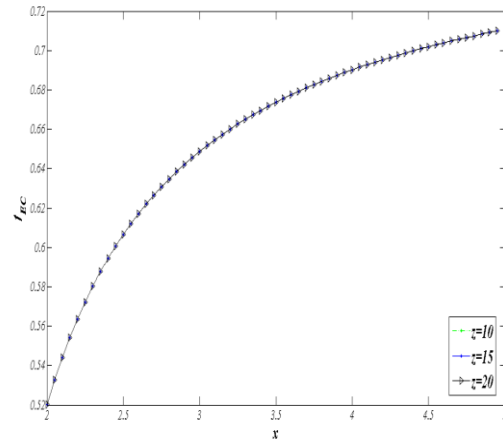


Figure 5. Fluid temperature ratio of (x) at various values of the sum of heat conductivity rate (z) on the power output in ($\tau = 5, y = 2$).

As shown in Fig. 6, by augmenting the fluid temperature ratio (x), the power output (W) enhances until the power output (W) is obtained, and subsequently, reduces by a rise in the fluid temperature ratio (x). It should be noticed that by increasing the sum of heat conductance rate (z), the heat entering the system increases, and as a result, the power output increases.

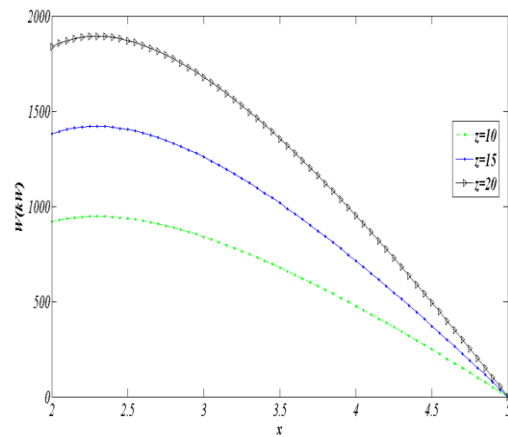


Figure 6. Fluid temperature ratio (x) at various values of the sum of heat conductivity rate (z) on the power output in ($\tau = 5, y = 2$).

4.1. Results of first scenario

By means of multi-objective optimization with the help of the NSGA-II method, the power output and the system's efficiency and dimensionless ecological-based thermo-economic function (f_E) are maximized all together. The design parameters of the optimization process are the fluid temperature ratio ($x = \frac{T_E}{T_C}$), parameter associated

with the heat conductance rate ($y = \frac{\alpha}{\beta}$), sum of heat conductance rate ($z = \alpha + \beta$), and temperature ratio (τ).

Figure 7 shows the frontier of optimum Pareto for the objective function power output and the system's first law efficiency and dimensionless ecological-based thermo-economic function (f_E), also the optimum outcomes associated with the decision-making methods. The change ranges of the results for the power output is 1139.792-2968.873 (kW) and 0.583-0.790 for efficiency, and for f_E is 0.022-0.046 (kW).

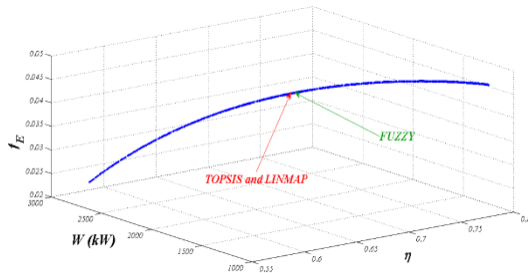


Figure 7. Pareto optimal frontier in the objectives' space for the first scenario.

The optimal outcomes provided for the objective functions and decision variables by the decision-making methods for the first scenario are listed in table 2. It illustrates the characteristics of the optimum solutions gained in the first scenario by the decision-making approaches. The deviation index is defined as:

$$d_+ = \sqrt{(\eta - \eta_n)^2 + (W - W_n)^2 + (f_E - f_{E,n})^2}$$

$$d_- = \sqrt{(\eta - \eta_{n,non-ideal})^2 + (W - W_{n,non-ideal})^2 + (f_E - f_{E,n,non-ideal})^2}$$

$$d = \frac{d_+}{(d_+) + (d_-)}$$

η_n , W_n , and $f_{E,n}$ indicate Euclidian of the first law efficiency, power output, and f_E .

A least deviation was obtained by the TOPSIS and LINMAP methods; consequently, the selected final optimum answer by these approaches was considered to be the optimum state of the heat engine in the first scenario.

Table 2. Decision-making of multi-objective optimal solutions for the first scenario.

Decision Making Method	Decision variables				Objectives			Deviation index from the ideal solution (d)
	x	z	y	τ	η	W	f_E	
TOPSIS	3.736	19.994	1.013	6.000	0.719	2379.814	0.039	0.322
LINMAP	3.7360	19.994	1.013	6.000	0.719	2379.814	0.039	0.322
Fuzzy	3.763	19.994	1.017	6.000	0.721	2357.833	0.039	0.334
Ideal solution	-	-	-	-	0.790	2968.873	0.046	0
Non-ideal solution	-	-	-	-	0.583	1139.729	0.022	∞

In order to assess the accuracy of the decision-making objectives, the mean absolute percentage error (MAPE) evaluation was employed. For the aim of measuring MAPE, 30 iterations of every

approach were carried out. Table 3 presents MAAE (maximum absolute percentage error) and MAPE of the aforementioned approaches.

Table 3. Error analysis based on the mean absolute percent error (MAPE) method for the first scenario.

Decision Making Method	TOPSIS			LINMAP			Fuzzy		
	η	W	f_E	η	W	f_E	η	W	f_E
Max Error %	0.038	0.048	0.032	0.041	0.051	0.032	4.992	6.926	2.589
Average Error %	0.028	0.036	0.022	0.029	0.036	0.022	3.352	4.651	1.738

4.2. Results of second scenario

The objective optimization functions in the second scenario comprising W, η , and dimensionless ecologico-economical (f_{EC}) (to be maximized) are explained by equations (3, 7, and 19). Figure 8 presents the Pareto optimal frontier for the second scenario optimization.

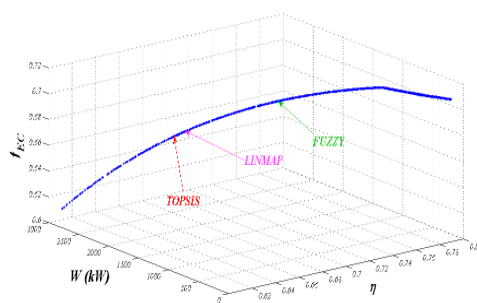


Figure 8. Pareto optimal frontier in the objectives' space for the second scenario.

Table 4 represents the optimum results in the second scenario. Also the deviation index can be calculated as follows:

$$d_+ = \sqrt{(\eta - \eta_n)^2 + (W - W_n)^2 + (f_{EC} - f_{EC,n})^2}$$

$$d_- = \sqrt{(\eta - \eta_{n,non-ideal})^2 + (W - W_{n,non-ideal})^2 + (f_{EC} - f_{EC,n,non-ideal})^2}$$

$$d = \frac{d_+}{(d_+) + (d_-)}$$

η_n , W_n , and $f_{EC,n}$ indicate the Euclidian form of the objectives. As the minimum deviation is obtained by the TOPSIS approach, it is considered as the final optimal solution for the thermal heat engine cycle in the second scenario.

Table 4. Decision-making of multi-objective optimal solutions for the second scenario.

Decision Making Method	Decision variables				Objectives			Deviation index from the ideal solution (d)
	x	z	y	τ	η	W	f_{EC}	
TOPSIS	3.375	19.992	1.027	6.000	0.689	2643.354	0.655	0.104
LINMAP	3.460	19.994	1.027	6.000	0.696	2586.464	0.658	0.123
Fuzzy	4.134	19.990	1.031	6.000	0.746	2034.523	0.681	0.310
Ideal solution	-	-	-	-	0.790	2950.314	0.710	0
Non-Ideal solution	-	-	-	-	0.609	1.904	0.610	∞

For the error analysis, MAPE was used. Hence, 30 iterations of every approach were carried out to provide an ultimate route by the decision-making

approaches. Table 5 illustrates the MAAE and MAPE results of the aforementioned decision-making methods.

Table 5. Error analysis based on the mean absolute percent error (MAPE) method for the second scenario.

Decision Making Method	TOPSIS			LINMAP			Fuzzy		
	η	W	f_{EC}	η	W	f_{EC}	η	W	f_{EC}
Max Error %	0.156	0.041	0.091	0.196	0.052	0.126	4.088	1.636	1.959
Average Error%	0.050	0.013	0.041	0.102	0.027	0.073	1.249	0.503	0.598

5. Conclusion

During this work, the thermodynamic analysis of an irreversible actual heat engine was carried out. The extra influences of the fluid temperature ratio, heat parameter, conductance rate, sum of heat conductance rate, and temperature ratio were taken into account in the assessment of the power, efficiency, dimensionless ecological-based thermo-economic function (f_E), and dimensionless ecologico-economical (f_{EC}) of the actual heat engine. Furthermore, the optimal state of the presented objective functions was determined. Through the applied multi-objective optimization process, four parameters including the fluid temperature ratio ($x = \frac{T_E}{T_C}$), parameter of the heat conductance rate ($y = \frac{\alpha}{\beta}$), sum of heat conductance rate ($z = \alpha + \beta$) and ratio of fluid temperature heat

source/sink, and ($\tau = \frac{T_H}{T_L}$) were considered as the decision characters. In order to determine a decisive solution from the results obtained with the help of multi-objective optimization, the decision-making techniques were implemented and the outputs were evaluated by the mean of error analysis. The coupled multi-objective evolutionary approaches (MOEAs) and non-dominated sorting genetic algorithm (NSGA-II) approach was presented. A comparison of the three prominent approaches LINAMP, TOPSIS, and FUZZY was performed in decision-making. Ultimately, the error analyses of the results were carried out. In the first scenario, the appropriate results were the result of the decisions made by TOPSIS and LINAMP with a deviation index equal to 0.322 from the ideal ratio of this scenario. In the second scenario, the

best decision-making results were achieved by the TOPSIS method with a deviation index equal to 0.104 from the ideal state for this scenario.

Nomenclature

E	Ecological function
\dot{W}	Power output
\dot{S}_{gen}	Entropy generation rate
f_E	Dimensionless ecological-based thermo-economic function
f_{EC}	Dimensionless ecologico-economical
η	First law efficiency of the system
TH	Heat source temperature
TL	Heat sink temperature
TC	Condenser temperature
T_E	Evaporator temperatures
T_0	Ambient temperature
\dot{Q}_H	Entering heat to the system
\dot{Q}_L	System heat rejection
α	Heat conductance of the hot side
β	Heat conductance of the cold side (kW/K)
I	Dimensionless internal irreversibility parameter
x	Ratio of fluid temperature ($x = \frac{T_E}{T_C}$)
y	Parameter of the heat conductance rate ($y = \frac{\alpha}{\beta}$)
z	Sum of heat conductance rate ($z = \alpha + \beta$)
τ	Temperature ratio
c1	Capital cost (\$/kW)
c2	Fuel cost (\$/kW)
c3	Environmental cost (\$/kW)
c4	
c5	Capital recovery factor multiplied by the investment cost per unit power output (\$/kW)
c6	Operation and maintenance cost (\$/kW)
F_E	Ecological-based thermo-economic function (kW/\$)
F_{EC}	Ecologico-economical function
F_{ij}^n	Matrix of objectives for different answers of the Pareto frontier
i	Index of each route on the Pareto frontier

References

[1] Ahmadi MH, Nazari MA, Sadeghzadeh M, Pourfayaz F, Ghazvini M, Ming T, et al. Thermodynamic and economic analysis of performance evaluation of all the thermal power plants: A review. Energy Sci Eng 2019; 7:30–65.

[2] Ahmadi MH, Banihashem SA, Ghazvini M, Sadeghzadeh M. Thermo-economic and exergy assessment and optimization of performance of a hydrogen production system by using geothermal energy. Energy Environ 2018; 29:1373–92.

[3] Ahmadi MH, Mohammadi O, Sadeghzadeh M, Pourfayaz F, Kumar R, Lorenzini G. Exergy and Economic Analysis of Solar Chimney in Iran Climate: Tehran, Semnan, and Bandar Abbas. Math Model Eng Probl 2020; 7:55–67.

[4] Ahmadi M, Sadaghiani M, Pourfayaz F, Ghazvini M, Mahian O, Mehrpooya M, et al. Energy and Exergy Analyses of a Solid Oxide Fuel Cell-Gas Turbine-Organic Rankine Cycle Power Plant with Liquefied Natural Gas as Heat Sink. Entropy 2018; 20:484.

[5] Mohammadi A, Ahmadi MH, Bidi M, Ghazvini M, Ming T. Exergy and economic analyses of replacing feedwater heaters in a Rankine cycle with parabolic trough collectors. Energy Reports 2018; 4:243–51.

[6] Assad MEH. Thermodynamic analysis of an irreversible MHD power plant. Int J Energy Res 2000; 24:865–75.

[7] Zhou S, Chen L, Sun F, Wu C. Cooling Load Density Optimization of an Irreversible Simple Brayton Refrigerator. Open Syst Inf Dyn 2002; 9:325–37.

[8] Nylund C, Assad MEH. Energy Optimization of Heat Engine with Infinite Heat Capacity Reservoirs 2013.

[9] Çengel YA, Boles MA. Thermodynamics: an engineering approach. McGraw-Hill; 2011.

[10] Novikov II. The efficiency of atomic power stations (a review). J Nucl Energy 1958;7:125–8.

[11] Curzon FL, Ahlborn B. Efficiency of a Carnot engine at maximum power output. Am J Phys 1975; 43:22–4.

[12] Ge Y, Chen L, Qin X, Xie Z. Exergy-based ecological performance of an irreversible Otto cycle with temperature-linear-relation variable specific heat of working fluid. Eur Phys J Plus 2017 1325 2017; 132:1–9.

[13] Vaudrey A, Lanzetta F, Feidt M. H. B. Reitlinger and the origins of the Efficiency at Maximum Power formula for Heat Engines. J Non-Equilibrium Thermodyn 2014; 39:199–203.

[14] Wu Z, Chen L, Ge Y, Sun F. Power, efficiency, ecological function and ecological coefficient of performance of an irreversible Dual-Miller cycle (DMC) with nonlinear variable specific heat ratio of working fluid. Eur Phys J Plus 2017 1325 2017; 132:1–

- 17.
- [15] Chen L, Ding Z, Zhou J, Wang W, Sun F. Thermodynamic performance optimization for an irreversible vacuum thermionic generator. *Eur Phys J Plus* 2017 1327 2017; 132:1–12.
- [16] Yin Y, Chen L, Wu F. Optimal power and efficiency of quantum Stirling heat engines. *Eur Phys J Plus* 2017 1321 2017; 132:1–10.
- [17] Xia S, Chen L, Sun F. Maximum cycle work output optimization for generalized radiative law Otto cycle engines. *Eur Phys J Plus* 2016 13111 2016; 131:1–14.
- [18] Madadi V, Tavakoli T, Rahimi A. Estimation of heat loss from a cylindrical cavity receiver based on simultaneous energy and exergy analyses. *J Non-Equilibrium Thermodyn* 2015; 40:49–61.
- [19] Angulo-Brown F. An ecological optimization criterion for finite-time heat engines. *J Appl Phys* 1991; 69:7465–9.
- [20] Yan Z. Comment on “an ecological optimization criterion for finite-time heat engines” [*J. Appl. Phys.* 69, 7465, (1991)]. *J Appl Phys* 1993; 73:3583.
- [21] Açikkalp E. Methods used for evaluation of actual power generating thermal cycles and comparing them. *Int J Electr Power Energy Syst* 2015; 69:85–9.
- [22] Açikkalp E. Exergetic sustainability evaluation of irreversible Carnot refrigerator. *Phys A Stat Mech Its Appl* 2015; 436:311–20.
- [23] Özel G, Ackkalp E, Savas AF, Yamk H. Novel thermoenvironmental evaluation criteria and comparing them for an actual heat engine. *Energy Convers Manag* 2015; 106:1118–23.
- [24] Özel G, Açikkalp E, Savaş AF, Yamk H. Comparative Analysis of Thermo-economic Evaluation Criteria for an Actual Heat Engine. *J Non-Equilibrium Thermodyn* 2016; 41:225–35.
- [25] J. Chen. The maximum power output and maximum efficiency of an irreversible Carnot heat engine. *J Phys D Appl Phys* 1994; 27:1144–9.
- [26] S Ozkaynak SG and HY. Finite-time thermodynamic analysis of a radiative heat engine with internal irreversibility. *J Phys D Appl Phys* 1994; 27:1139–43.
- [27] C. Cheng and C. Chen. The ecological optimization of an irreversible Carnot heat-engine. *J Phys D Appl Phys* 1997; 30:1602–9.
- [28] Xia D, Chen L, Sun F, Wu C. Universal ecological performance for endo-reversible heat engine cycles. *Int J Ambient Energy* 2006; 27:15–20.
- [29] Chen L, Zhou J, Sun F, Wu C. Ecological optimization for generalized irreversible Carnot engines. *Appl Energy* 2004; 77:327–38.
- [30] Zhu X, Chen L, Sun F, Wu C. Exergy-based ecological optimization for a generalized irreversible Carnot refrigerator. *J Energy Inst* 2006; 79:42–6.
- [31] Ibrahim DM, Klein SA, Mitchell JW. Optimum heat power cycles for specified boundary conditions. *J Eng Gas Turbines Power* 1991; 113:514–21.
- [32] De Vos A. Endoreversible economics. *Energy Convers Manag* 1997; 38:311–7.
- [33] Sahin B, Kodal A. Finite time thermoeconomic optimization for endoreversible refrigerators and heat pumps. *Energy Convers Manag* 1999; 40:951–60.
- [34] Sadatsakkak SA, Ahmadi MH, Ahmadi MA. Thermodynamic and thermo-economic analysis and optimization of an irreversible regenerative closed Brayton cycle. *Energy Convers Manag* 2015; 94:124–9.
- [35] Ahmadi MH, Ahmadi MA, Bayat R, Ashouri M, Feidt M. Thermo-economic optimization of Stirling heat pump by using non-dominated sorting genetic algorithm. *Energy Convers Manag* 2015; 91:315–22.
- [36] Ahmadi MH, Ahmadi MA, Mehrpooya M, Hosseinzade H, Feidt M. Thermodynamic and thermo-economic analysis and optimization of performance of irreversible four-temperature-level absorption refrigeration. *Energy Convers Manag* 2014; 88:1051–9.
- [37] Ahmadi MH, Sayyaadi H, Mohammadi AH, Barranco-Jimenez MA. Thermo-economic multi-objective optimization of solar dish-Stirling engine by implementing evolutionary algorithm. *Energy Convers Manag* 2013; 73:370–80.
- [38] Barranco-Jiménez MA, Sánchez-Salas N. Effect of combined heat transfer on the thermoeconomic performance of an irreversible solar-driven heat engine at maximum ecological conditions. Vol. 59. 2013.
- [39] Chen L, Sun F, Wu C. Thermo-economics for endoreversible heat-engines. *Appl Energy* 2005; 81:388–96.
- [40] Chen L, Xiaoqin Z, Sun F, Wu C. Exergy-based ecological optimization for a generalized irreversible Carnot heat-pump. *Appl Energy* 2007; 84:78–88.
- [41] Chen L, Zhang W, Sun F. Power, efficiency, entropy-generation rate and ecological optimization for a class of generalized irreversible universal heat-engine cycles. *Appl Energy* 2007; 84:512–25.
- [42] Ust Y, Sahin B, Sogut OS. Performance analysis and optimization of an irreversible dual-cycle based on an ecological coefficient of performance criterion. *Appl Energy* 2005;82:23–39.
- [43] Ust Y, Sahin B. Performance optimization of irreversible refrigerators based on a new thermo-ecological criterion. *Int J Refrig* 2007; 30:527–34.
- [44] Ust Y, Sahin B, Kodal A, Akcay IH. Ecological coefficient of performance analysis and optimization of an irreversible regenerative-Brayton heat engine. *Appl Energy* 2006; 83:558–72.
- [45] Ust Y, Akkaya A V., Safa A. Analysis of a vapour

compression refrigeration system via exergetic performance coefficient criterion. *J Energy Inst* 2011; 84:66–72.

[46] Akkaya AV, Sahin B, Huseyin Erdem H. An analysis of SOFC/GT CHP system based on exergetic performance criteria. *Int J Hydrogen Energy* 2008; 33:2566–77.

[47] Mironova VA, Tsirlin AM, Kazakov VA, Berry RS. Finite-time thermodynamics: Exergy and optimization of time-constrained processes. *J Appl Phys* 1994; 76:629–36.

[48] Andresen B, Rubin MH, Berry RS. Availability for finite-time processes. General theory and a model. *J Phys Chem* 1983; 87:2704–13.

[49] Blecic I, Cecchini A, Trunfio GA. A decision support tool coupling a causal model and a multi-objective genetic algorithm. *Appl Intell* 2007; 26:125–37.

[50] Ombuki B, Ross BJ, Hanshar F. Multi-objective genetic algorithms for vehicle routing problem with time windows. *Appl Intell* 2006; 24:17–30.

[51] Özyer T, Zhang M, Alhadj R. Integrating multi-objective genetic algorithm based clustering and data partitioning for skyline computation. *Appl Intell* 2011; 35:110–22.

[52] Van Veldhuizen DA, Lamont GB. Multiobjective evolutionary algorithms: analyzing the state-of-the-art. *Evol Comput* 2000; 8:125–47.

[53] Ahmadi MH, Hosseinzade H, Sayyaadi H, Mohammadi AH, Kimiaghdam F. Application of the multi-objective optimization method for designing a powered Stirling heat engine: Design with maximized power, thermal efficiency and minimized pressure loss. *Renew Energy* 2013; 60:313–22.

[54] Ahmadi MH, Dehghani S, Mohammadi AH, Feidt M, Barranco-Jimenez MA. Optimal design of a solar driven heat engine based on thermal and thermo-economic criteria. *Energy Convers Manag* 2013; 75:635–42.

[55] Ahmadi MH, Sayyaadi H, Dehghani S, Hosseinzade H. Designing a solar powered Stirling heat engine based on multiple criteria: Maximized thermal efficiency and power. *Energy Convers Manag* 2013; 75:282–91.

[56] Ahmadi MH, Ahmadi MA, Mohammadi AH, Mehrpooya M, Feidt M. Thermodynamic optimization of Stirling heat pump based on multiple criteria. *Energy Convers Manag* 2014; 80:319–28.

[57] Ahmadi MH, Ahmadi MA, Mohammadi AH, Feidt M, Pourkiaei SM. Multi-objective optimization of an irreversible Stirling cryogenic refrigerator cycle. *Energy Convers Manag* 2014; 82:351–60.

[58] Ahmadi MH, Mohammadi AH, Dehghani S. Evaluation of the maximized power of a regenerative endoreversible Stirling cycle using the thermodynamic analysis. *Energy Convers Manag* 2013; 76:561–70.